

Abstract. We propose a vacuum gap (VG) model which can be applied uniformly for normal and high magnetic field pulsars. The model requires strong and non-dipolar surface magnetic field near the pulsar polar cap. We assume that the actual surface magnetic field \mathbf{B}_s in pulsars results from a superposition of global dipole field \mathbf{B}_d and crust-anchored small scale magnetic anomaly \mathbf{B}_m . We provide a numerical formalism for modelling such structures of surface magnetic field and explore it within the framework of VG model, which requires strong surface fields $B_s \gtrsim 10^{13}$ G. Thus, in order to increase the resultant surface field to values exceeding 10^{13} G, in low magnetic field pulsars with $B_d \ll 10^{13}$ G it is required that $B_m \gg B_d$, with the same polarities (orientations) of \mathbf{B}_d and \mathbf{B}_m . However, if the polarities are opposite, the resultant surface field can be lower than the dipolar surface component inferred from the pulsar spin-down. We propose that high magnetic field pulsars (HBPs) with the inferred global dipole field B_d exceeding the so called photon splitting threshold $B_{cr} \sim 4 \times 10^{13}$ G, can generate observable radio emission ‘against the odds’, provided that the surface dipolar magnetic field B_d is reduced below B_{cr} by the magnetic anomaly B_m of the right strength and polarity. We find that the effective reduction is possible if the values of B_d and B_m are of the same order of magnitude, which should be expected in HBPs with $B_d > B_{cr}$. The proposed VG model of radio emission from HBPs, in which pair production occurs right above the polar cap, is an alternative to the recently proposed lengthened space charge limited flow (SCLF) model, in which pair formation front is located at relatively high altitudes, where the dipole field is degraded below B_{cr} . Our model allows high B_d radio-loud pulsars not only just above B_{cr} but even above 2×10^{14} G, which is the upper limit for HBPs within the lengthened SCLF model.

Key words: pulsars: magnetic fields, radio-emission

Modelling of surface magnetic field in neutron stars: application to radio pulsars

Janusz A. Gil¹, George I. Melikidze^{1,2}, and Dipanjan Mitra³

¹ Institute of Astronomy, University of Zielona Góra, Lubuska 2, 65-265, Zielona Góra, Poland

² Center for Plasma Astrophysics, Abastumani Astrophysical Observatory, Al.Kazbegi ave. 2a, Tbilisi 380060, Georgia

³ Max-Planck Institute for Radioastronomy, Auf dem Hügel 69, D-53121, Bonn, Germany

Received / Accepted

1. Introduction

The properties of radio emission of typical pulsars strongly suggest that the magnetic field is purely dipolar, at least at altitudes r of several stellar radii $R = 10^6$ cm, where the radio emission is expected to originate (e.g. Kijak & Gil, 1997, 1998, and references therein). However, this may not be a good description of the structure of the magnetic field at the stellar surface. In fact, already Ruderman & Sutherland (RS75) implicitly assumed that the radius of curvature of field lines above the polar cap should be about 10^6 cm, which is inconsistent with the global dipolar magnetic field. Several authors argued on theoretical grounds that the magnetic field could be produced by currents flowing in thin crustal layers of the neutron star, which would generate non-dipolar fields at the surface (e.g. Blandford, Applegate & Hernquist, 1983; Krolik, 1991; Ruderman, 1991; Arons, 1993; Chen & Ruderman, 1993; Geppert & Urpin, 1994; Mitra, Konar & Bhattacharya, 1999). A lot of observational evidence has also been presented. Page & Sarmiento (1990) and Bulik et al. (1992, 1995) reported that interpretation of their analysis of X-ray pulsars suggested small scale magnetic anomalies on the polar cap, which would strongly deviate the surface field from the purely dipolar configuration. It is believed that thermal X-rays from the polar cap surface are good diagnostic tool to infer the structure of the surface magnetic field. Several similar arguments in favour of non-dipolar nature of surface magnetic field can also be found in Becker & Trümper (1997); Cheng, Gil & Zhang (1998); Rudak & Dyks (1999); Cheng & Zhang (1999); Thompson & Duncan (1995, 1996), and Murakami et al. (1999), and Tauris & Konar (2001).

Woltjer (1964) proposed that the magnetic field is the fossil field of the progenitor star amplified during the collapse and anchored in the superfluid core of the neutron star. We will assume in this paper that the magnetic field was also generated in the outer crust during or shortly after the neutron star was formed by some unspecified mechanism (e.g. thermomagnetic instabilities; Blandford, Applegate & Hernquist, 1983). Urpin, Levshakov & Iakovlev

(1986) showed that in the crustal model it is only possible to form small scale surface field anomalies with a typical size of the order of 100 meters. Gil & Mitra (2001) demonstrated that such ‘sunspot’ like magnetic field structures on the polar cap surface help to sustain VG-driven radio emission of pulsars. Here we envisage the scenario where the magnetic field of neutron star is non-dipolar in nature as a superposition of the fossil field in the core and the crustal field structures. The crust gives rise to small scale anomalies which can be modelled by a number of crust anchored dipoles oriented in different directions (e.g. Blandford, Applegate & Hernquist, 1983; Arons, 1993). The superposition of global dipole and local anomaly is illustrated in Fig. 1, where for clarity of presentation only one local, crust associated dipole is marked.

Formation of dense electron-positron pair plasma is essential for pulsar radiation, especially (but not only) at radio wavelengths. Purely quantum process for magnetic pair production $\gamma \rightarrow e^-e^+$ is commonly invoked as a source of this plasma (e.g. Sturrock, 1971; Ruderman & Sutherland, 1975). However, at superstrong magnetic fields close to the so-called quantum field $B_q = 4.4 \times 10^{13}$ G, the process of free e^-e^+ pair production can be dominated by the phenomenon of photon splitting (Adler et al., 1970; Bialynicka & Bialynicki et al., 1970; Baring & Harding, 1998) and/or bound positronium formation (Usov & Melrose, 1995, 1996). While the latter process can reduce the number of free pairs at magnetic fields $B \gtrsim 0.1B_q$ (e.g. Baring & Harding, 2001), the former one can entirely suppress the magnetic pair production at $B \gtrsim 10^{13}$ G, provided that photons polarized both parallel and perpendicular to local magnetic field direction can split (e.g. Baring, 2001; Baring & Harding, 2001). This assumption will be implicitly kept throughout this paper. Under these circumstances one can roughly define a photon splitting critical line $B_{cr} \sim B_q$ and expect that there should be no radio pulsar above this line on the $B_d - P$ diagram, where $B_d = 6.4 \times 10^{19}(P\dot{P})^{1/2}$ G is the dipole surface magnetic field estimated at the pole from the pulsar period P and its derivative \dot{P} (Shapiro & Teukolsky, 1983; Usov & Melrose, 1996). This death-line

is more illustrative than quantitative. In fact, a number of specific model dependent death-lines separating radio-loud from radio-quiet pulsars are available in the literature (Baring & Harding, 1998, 2001; Zhang & Harding, 2000a, 2001). All these slightly period dependent death-lines cluster around B_q on the $B_d - P$ diagram, and hence the quantum field is conventionally treated as a threshold magnetic field above which pulsar radio emission ceases. In this paper we also use this terminology, bearing in mind that the photon splitting threshold realistically means a narrow range of magnetic fields around the critical quantum field $B_q \sim 4 \times 10^{13}$ G, certainly above 10^{13} G (see review by Baring, 2001). For convenience, in all numerical examples presented in Figs. 2-6 and subsequent discussions we assume the threshold magnetic field $B_{cr} = B_q$.

In order to produce the necessary dense electron-positron plasma, high voltage accelerating region has to exist near the polar cap of pulsars. Two models of such acceleration regions were proposed: stationary space charge limited flow (SCLF) models (Sharleman, Arons & Fawley, 1978; Arons & Sharleman, 1979; Arons, 1981) in which charged particles flow freely from the polar cap, and highly non-stationary vacuum gap (VG) models (Ruderman & Sutherland, 1975; Cheng & Ruderman, 1977, 1980; Gil & Mitra, 2001) in which the free outflow of charged particles from the polar cap surface is strongly impeded. In the VG models the charged particles accelerate within a height scale of about polar cap radius of $\sim 10^4$ cm, due to high potential drop across the gap, while in the SCLF models particles accelerate within a height scale of a stellar radius $\sim 10^6$ cm, due to the potential drop resulting from the curvature of field lines and/or inertia of outstreaming particles. In both models the free e^-e^+ pairs are created if the kinematic threshold $\varepsilon_\gamma \cdot \sin \theta_t = 2mc^2$ is reached or exceeded and the local magnetic field is lower than the photon splitting threshold $B \sim B_{cr}$, where $\varepsilon_\gamma = \hbar\omega$ is the photon energy and θ_t is the propagation angle with respect to the direction of the local magnetic field.

Recent discovery of high magnetic field pulsars (HBPs) however has challenged the existing pair creation theories. A few HBPs found the inferred surface dipolar fields above the photon splitting level: PSRs J1119–6127, J1814–1744 and J1726–3530 (Table 1). Moreover, yet another strong field neutron star PSR J1846–0258 with $B_d \sim 5 \times 10^{13}$ G was discovered (Gotthelf et al., 2000), which seems to be radio-quiet (Kaspi et al., 1996), although its X-ray emission is apparently driven by dense e^-e^+ pair plasma (e.g. Cordes, 2001). However, one should keep in mind that the actual threshold due to photon splitting and/or bound positronium formation can be well below the critical field $B_{cr} \sim 4 \times 10^{13}$ G, indicating that all high magnetic field radio pulsars with $B_d > 10^{13}$ G pose a challenge. To evade the photon splitting problem for these pulsars Zhang & Harding (2000a, ZH00 hereafter) proposed “a unified picture for HBPs and magnetars”. They argued that radio-quiet magnetars cannot have active inner accel-

Table 1. Radio-loud HBPs with inferred magnetic field $B_d = 6.4 \times 10^{19}(P\dot{P})^{1/2}$ G higher than critical quantum field $B_{cr} = 4.4 \times 10^{13}$ G (after Table 1 in Zhang & Harding, 2000b)

source	P (s)	\dot{P} (s/s)	B_d (G)
PSR J1814–1744	3.98	7.43×10^{-13}	1.1×10^{14}
PSR J1119–6127	0.41	4.02×10^{-12}	8.2×10^{13}
PSR J1726–3530	1.11	1.22×10^{-12}	7.4×10^{13}

erators (thus no e^-e^+ pair production), while the HBPs can, with a difference attributed to the relative orientations of rotation and magnetic axes (neutron stars can be either parallel rotator (PRs) with $\Omega\mathbf{B}_d > 0$ or antiparallel rotator (APRs) with $\Omega\mathbf{B}_d < 0$, where Ω is the pulsar spin axis and \mathbf{B}_d is the magnetic field at the pole). If the photon splitting suppresses completely the pair production at the polar cap surface, then the VG inner accelerator cannot form, since the high potential drop cannot be screened at the top of the acceleration region. Hence, ZH00 argued that in high magnetic field regime ($B_d > B_{cr}$) the pair production process is possible only if the SCLF accelerator forms. In fact, such SCLF accelerators are typically quite long and their pair formation front (PFF) can occur at high altitudes r , where the dipolar magnetic field $B_d \propto r^{-3}$ has degraded below the critical value B_{cr} . Furthermore, ZH00 demonstrated that such lengthened SCLF accelerator in magnetar environment can form only for PRs and not for APRs. Consequently they concluded that the radio-loud HBPs are PRs with developed lengthened SCLF accelerator, while the radio-quiet magnetars (AXPs and SGRs) represent APRs. It is worth emphasizing here that ZH00 developed their model under the assumption that the magnetic field at the surface of HBPs is purely dipolar.

In this paper we propose an alternative model for radio-loud HBPs based on highly non-dipolar surface magnetic field, in which the photon splitting within the VG inner acceleration region does not operate even if the dipole magnetic field exceeds the critical value B_{cr} at the polar cap. Thus our model requires that HBPs are APRs, which is a consequence of the VG scenario (e.g. Ruderman & Sutherland, 1975; Gil & Mitra, 2001). This model is a follow-up work of Gil & Mitra (2001), who argued that the VG can form if the actual surface magnetic field is about 10^{13} Gauss. In other words, they assumed that all VG-driven radio pulsars have a very strong, highly non-dipolar surface magnetic field, with a strength more or less independent of the value of the global dipole field inferred from the magnetic breaking law. Thus, if $B_d \ll 10^{13}$ G then $B_s \gg B_d$ and if $B_d \gtrsim 10^{13}$ G then $B_s \sim B_d$; however, in any case $B_s < B_{cr} \sim B_q$. We argue that such strong surface field anomalies can increase low dipolar field $B_d \ll B_{cr}$ in normal pulsars to values exceeding 10^{13} G (required by conditions for VG formation - see Gil & Mi-

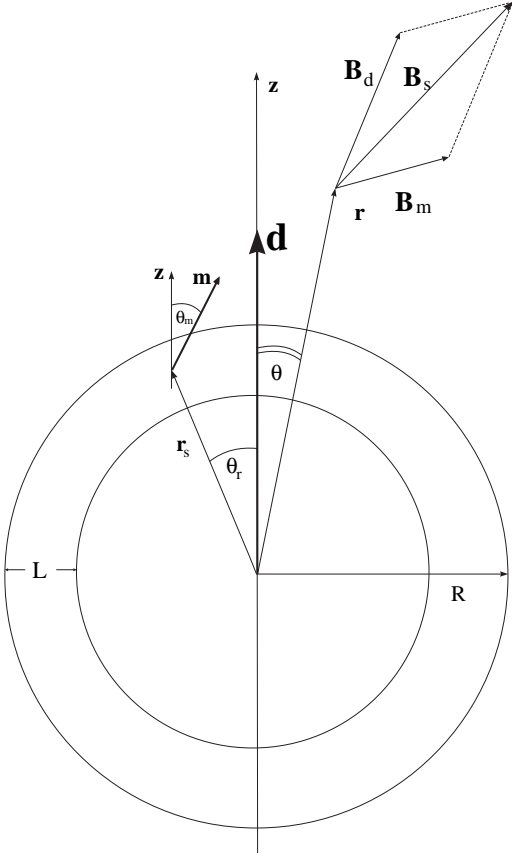


Fig. 1. Superposition of the star centered global magnetic dipole \mathbf{d} and crust anchored local dipole \mathbf{m} placed at $\mathbf{r}_s = (r_s \sim R, 0 = \theta_r)$ and inclined to the z -axis by an angle θ_m . The actual surface magnetic field at radius vector $\mathbf{r} = (r, \theta)$ is $\mathbf{B}_s = \mathbf{B}_d + \mathbf{B}_m$, where $\mathbf{B}_d = 2\mathbf{d}/r^3$, $\mathbf{B}_m = 2\mathbf{m}/|\mathbf{r} - \mathbf{r}_s|$, r is the radius (altitude) and θ is the polar angle (magnetic colatitude). R is the radius of the neutron star and L is the crust thickness.

tra 2001) if global and local surface fields have the same polarities, or reduce very high dipolar field $B_d \gtrsim B_{cr}$ in HBPs if both these components are of comparable values and have opposite polarities.

2. Modelling the Surface Magnetic Field

We model the actual surface magnetic field by superposition of the star centered global dipole \mathbf{d} and a crust anchored dipole moment \mathbf{m} , whose influence results in small scale deviations of surface magnetic field from the global dipole. According to general situation presented in Fig. 1

$$\mathbf{B}_s = \mathbf{B}_d + \mathbf{B}_m, \quad (1)$$

where

$$\mathbf{B}_d = \left(\frac{2d \cos \theta}{r^3}, \frac{d \sin \theta}{r^3}, 0 \right), \quad (2)$$

r and θ are star-centered polar co-ordinates, and

$$\mathbf{B}_m = \frac{3(\mathbf{r} - \mathbf{r}_s)(\mathbf{m} \cdot (\mathbf{r} - \mathbf{r}_s)) - \mathbf{m}|\mathbf{r} - \mathbf{r}_s|^2}{|\mathbf{r} - \mathbf{r}_s|^5}. \quad (3)$$

The global magnetic dipole moment $d = (1/2)B_d R^3$, where $B_d = 6.4 \cdot 10^{19} (P \cdot \dot{P})^{1/2}$ G is the dipole component at the pole derived from the pulsar spin-down rate, and the crust anchored local dipole moment $m = (1/2)B_m \Delta R^3$, where $\Delta R \sim 0.05R$ is the characteristic crust dimension ($R = 10^6$ cm). We use spherical coordinates with z axis directed along the global magnetic dipole moment \mathbf{d} . Thus, $\mathbf{r}_s = (r_s, \theta_r, \phi_r)$ and $\mathbf{m} = (m, \theta_m, \phi_m)$.

To obtain the equation of the open magnetic field lines we first define the boundary of the open field lines at an altitude where the magnetic field should be a pure dipole and we have chosen as a starting altitude $r = 50R$. Then we solve the system of differential equations

$$\frac{d\theta}{dr} = \frac{B_\theta^d + B_\theta^m}{r(B_r^d + B_r^m)} \equiv \Theta_1, \quad (4)$$

$$\frac{d\phi}{dr} = \frac{B_\phi^m}{r(B_r^d + B_r^m) \sin \theta} \equiv \Phi_1, \quad (5)$$

with the initial conditions $\mathbf{B}_m = 0$ defined at $r = 50R$ (already at $r = 5R$ the ratio $B_m/B_d \sim 10^{-4}$) and trace the field lines down to the stellar surface ($r = R$). Here

$$B_r^m = -\frac{1}{D^{2.5}} (3Tr_r^s - 3Tr + Dm_r),$$

$$B_\theta^m = -\frac{1}{D^{2.5}} (3Tr_\theta^s + Dm_\theta),$$

$$B_\phi^m = -\frac{1}{D^{2.5}} (3Tr_\phi^s + Dm_\phi) \quad (6)$$

and

$$D = r_s^2 + r^2$$

$$- 2r_s r (\sin \theta_r \sin \theta \cos(\phi - \phi_r) + \cos \theta_r \cos \theta),$$

$$T = m_r r - (m_r r_r^s + m_\theta r_\theta^s + m_\phi r_\phi^s),$$

$$r_r^s = r_s (\sin \theta_r \sin \theta \cos(\phi - \phi_r) + \cos \theta_r \cos \theta),$$

$$r_\theta^s = r_s (\sin \theta_r \cos \theta \cos(\phi - \phi_r) - \cos \theta_r \sin \theta),$$

$$r_\phi^s = -r_s \sin \theta_r \sin(\phi - \phi_r)$$

$$m_r = m (\sin \theta_m \sin \theta \cos(\phi - \phi_m) + \cos \theta_m \cos \theta),$$

$$m_\theta = m (\sin \theta_m \cos \theta \cos(\phi - \phi_m) - \cos \theta_m \sin \theta),$$

$$m_\phi = -m \sin \theta_m \sin(\phi - \phi_m). \quad (7)$$

The curvature $\rho_c = 1/\mathfrak{R}$ of the field lines (where \mathfrak{R} is the radius of curvature presented for various cases in Fig.8) is calculated as

$$\rho_c = \left(\frac{ds}{dr} \right)^{-3} \left| \left(\frac{d^2 \mathbf{r}}{dr^2} \frac{ds}{dr} - \frac{d\mathbf{r}}{dr} \frac{d^2 s}{dr^2} \right) \right|, \quad (8)$$

or

$$\rho_c = (S_1)^{-3} (J_1^2 + J_2^2 + J_3^2)^{1/2}, \quad (9)$$

where

$$\frac{ds}{dr} = \sqrt{(1 + r^2 \Theta_1^2 + r^2 \Phi_1^2 \sin^2 \theta)},$$

$$J_1 = X_2 S_1 - X_1 S_2, \quad J_2 = Y_2 S_1 - Y_1 S_2,$$

$$J_3 = Z_2 S_1 - Z_1 S_2$$

$$X_1 = \sin \theta \cos \phi + r \Theta_1 \cos \theta \cos \phi - r \Phi_1 \sin \theta \sin \phi,$$

$$Y_1 = \sin \theta \sin \phi + r \Theta_1 \cos \theta \sin \phi + r \Phi_1 \sin \theta \cos \phi,$$

$$Z_1 = \cos \theta - r \Theta_1 \sin \theta,$$

$$X_2 = (2\Theta_1 + r\Theta_2) \cos \theta \cos \phi - (2\Phi_1 + r\Phi_2) \sin \theta \sin \phi \\ - r(\Theta_1^2 + \Phi_1^2) \sin \theta \cos \phi - 2r\Theta_1 \Phi_1 \cos \theta \sin \phi,$$

$$\begin{aligned}
 Y_2 &= (2\Theta_1 + r\Theta_2) \cos \theta \sin \phi + (2\Phi_1 + r\Phi_2) \sin \theta \cos \phi \\
 &\quad - r(\Theta_1^2 + \Phi_1^2) \sin \theta \sin \phi + 2r\Theta_1\Phi_1 \cos \theta \cos \phi, \\
 Z_2 &= -\Theta_1 \sin \theta - \Theta_1 \sin \theta - r\Theta_2 \sin \theta - r\Theta_1^2 \cos \theta, \\
 S_1 &= \sqrt{1 + r^2\Theta_1^2 + r^2\Phi_1^2 \sin^2 \theta}, \\
 S_2 &= S_1^{-1} (r\Theta_1^2 + r^2\Theta_1\Theta_2 + r\Phi_1^2 \sin^2 \theta \\
 &\quad + r^2\Phi_1\Phi_2 \sin^2 \theta + r^2\Theta_1\Phi_1^2 \sin \theta \cos \theta), \\
 \Theta_2 &= \frac{d\Theta_1}{dr}, \quad \Phi_2 = \frac{d\Phi_1}{dr}. \tag{10}
 \end{aligned}$$

For simplicity, in this paper we mostly consider an axially symmetric case in which both \mathbf{d} and \mathbf{m} are directed along z -axis (parallel or antiparallel), thus $\theta_r = \theta_m = \phi_r = \phi_m = 0$. Also, for convenience, \mathbf{m} is expressed in units of \mathbf{d} . We use normalized units in which $d = P = R = 1$ and $r_s = 0.95$. (see caption of Fig. 2 for the normalization convention). All calculations are carried out in three-dimensions, although, for clarity of graphic presentation, in figures we present only two-dimensional cuts of the open field line regions.

2.1. High magnetic field pulsars

As mentioned above, the formation of VG inner accelerator requires very high magnetic field $B \gtrsim 10^{13}$ G on the surface of the polar cap (Usov & Melrose, 1995, 1996; Gil & Mitra, 2001). This can be achieved not only in pulsars with high dipolar field $B_d \gtrsim 10^{13}$ G. In fact, some of the low field pulsars with $B_d \ll 10^{13}$ G can have surface field $B_s \gtrsim 10^{13}$ G if $B_m \gg B_d$ (thus $m \gg 1.25 \times 10^{-4} d$). We discuss such normal, low field pulsars later in this paper. Presently let us consider the HBP with a dipolar surface field at the pole $B_d = 6.4 \times 10^{19} (P \cdot \dot{P})^{1/2}$ G exceeding the photon splitting limit $B_{cr} \sim B_q$. If all photon splitting modes operate, such pulsar should be radio-quiet. Alternatively these pulsars could be radio-loud if the effective surface field is reduced below B_{cr} . Such scenario can be achieved if the polarities of magnetic moments \mathbf{d} and \mathbf{m} are opposite, that is \mathbf{d} and \mathbf{m} are antiparallel. Fig. 2 presents a case with $\mathbf{m} = -10^{-4} \mathbf{d}$ and $\Delta R/R = 0.05$. The actual surface values of $B^s = \sqrt{(B_r^s)^2 + (B_\theta^s)^2}$ as well as radial components of $B_r^s = \mathbf{B}_s \cdot \mathbf{R}/R$ and $B_r^d = \mathbf{B}_d \cdot \mathbf{R}/R$ are presented in the lower panel of Fig. 2 (note that all radial components are positive and that the total B^s is almost equal B_r^s in this case). At the pole (radius $r = R$ and polar angle $\theta = 0$) the ratio $B_m/B_d = (m/d) \cdot (R/\Delta R)^3 = 0.8$ and thus $B_s = B_d - B_m = B_d(1 - 0.8) = 0.2B_d$. As one can see from this figure, all surface field lines between $-\theta_s$ and $+\theta_s$ are open, but the ratio B_s/B_d increases towards the polar cap edge, reaching the value of about 0.5 in the region between polar angles $|\theta_d|$ and $|\theta_s|$. The ratio B_m/B_d is also about 0.5 in this region. Thus, the global dipolar field ($B_d = 2$ in our units) is effectively reduced between 2 and 5 times in different parts of the polar cap (defined as the surface area from which the open magnetic field lines emanate). This means that the ratio B_m/B_d ranges from

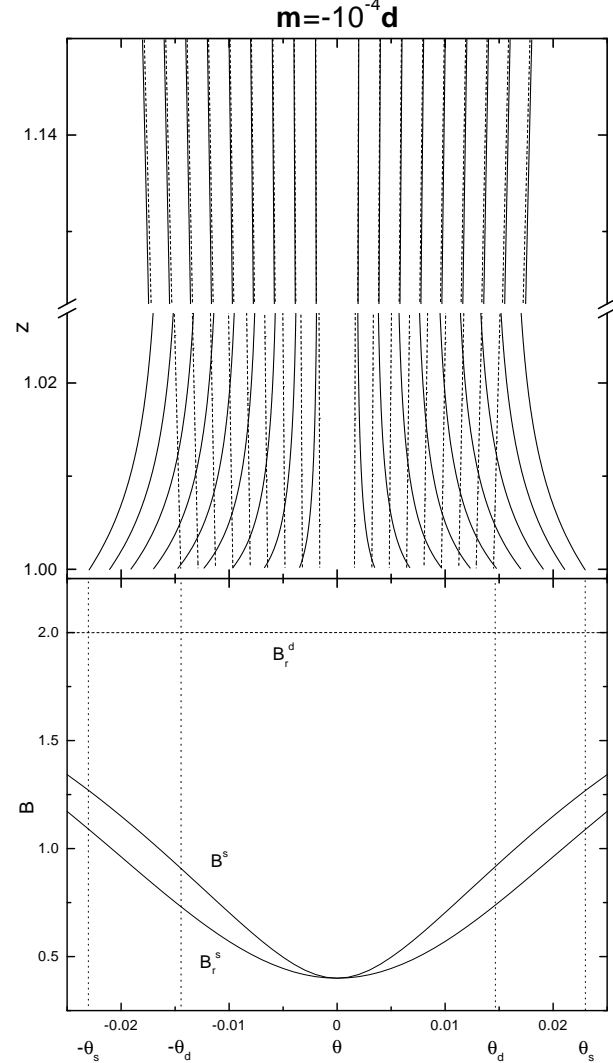


Fig. 2. Structure of surface magnetic field for a superposition of the global star centered dipolar moment \mathbf{d} and crust anchored dipole moment $\mathbf{m} = -10^{-4} \mathbf{d}$ (Fig. 1). The open dipolar field lines (solid) and the actual surface open field lines (dashed) are shown in the upper panel. The horizontal axis is labelled by an azimuthal angle θ (magnetic colatitude), which measures the polar cap radius. For purely dipolar field lines the polar cap radius $r_d \approx R \cdot \sin \theta_d$, which for pulsar period $P = 1$ s is about 0.014 radians (thus $r_d \approx 1.4 \cdot 10^4$ cm). The actual polar cap is broader with the last open lines emanating at the polar angles $\theta_s \approx 0.023$ (thus the actual polar cap radius $r_s = 2.3 \cdot 10^4$ cm = $1.65r_d$). The actual open surface field lines (solid) reconnect with dipolar ones (dashed) at distances $z = (r/R) \cdot \cos \theta \approx 1.2$, where r is the radius and $\theta < 0.025$ radians. In the lower panel the surface values ($r = R$) of both dipolar field (dashed horizontal) and the actual field (solid line) are shown. The radial components $B_r^d = 2d \cos \theta / R^3 \approx 2$ and $B_r^s = (\mathbf{B}_d + \mathbf{B}_m) \cdot \mathbf{r}/r$, and total values $B_s = \sqrt{(B_r^s)^2 + (B_\theta^s)^2}$ are presented (where $d = R = 1$ is assumed for convenience).

0.5 to 0.8 across the polar cap. The actual polar cap is broader than the canonical dipolar polar cap (two dashed vertical lines correspond to last open dipolar field lines emanating at the polar angles $\theta_d = \pm 0.014$ radians for typical period $P = 1$ s). The ratio of actual to dipolar polar cap radii is $\theta_s/\theta_d \sim 5/3$ in this case. Thus, using the argument of magnetic flux conservation of the open field lines, one can say that an effective surface magnetic field of the polar cap is about 2.8 times lower than the dipolar surface field measured from the values of P and \dot{P} . If the estimated dipole field $B_d^p \approx 10^{14}$ G (like in the case of PSR J1814–1744, Table 1) then the actual surface field at the pole is only $B_s \sim 2.5 \cdot 10^{13}$ G, well below the photon splitting death line $B_{cr} = 4.4 \times 10^{13}$ G. Such pulsar can be radio-loud without invoking the lengthened SCLF accelerator proposed by ZH00. As shown by Gil & Mitra (2001), in such strong surface magnetic field the vacuum gap accelerator can form, which implies low altitude coherent radio emission (Melikidze, Gil & Pataraya, 2000, see section 3 in this paper) at altitudes $r_{em} \sim 50R$ (for a typical pulsar with $P = 1$ s) in agreement with observational constraints on radio emission altitudes (Cordes, 1978, 1992; Kijak & Gil, 1997, 1998; Kijak, 2001).

Fig. 3 presents another case of opposite polarities $\mathbf{m} = -2 \times 10^{-4}\mathbf{d}$, with a magnitude of \mathbf{m} two times stronger than in the previous case (Fig. 2). Again for $\Delta R/R \sim 0.05$, $B_m/B_d = (m/d)(R/\Delta R)^3 = 1.6$ at the pole ($r = R$ and $\theta = 0$) and $B_s = B_d - B_m = -0.6B_d$. The negative sign of the ratio B_s/B_d means that the surface magnetic field \mathbf{B}_s is directed opposite to \mathbf{B}_d near the pole, that is the circumpolar field lines with polar angles $-\theta_{s1} < \theta < \theta_{s1}$ (where $\theta_{s1} \sim 0.031$) are closed. The last open surface field lines (solid) emanating at polar angles $\theta_s = \pm\theta_{s2}$ (where $\theta_{s2} \sim 0.037$) reconnect with last open dipolar field lines (dashed) at altitudes $z \sim 1.2$ (thus about 2 km above the surface). The actual polar cap, which is the surface through which the open magnetic field lines emanate, has a shape of a ring ($0.031 \lesssim |\theta_s| \lesssim 0.037$) located outside the circle of dipolar polar cap with angular radius $\theta_d = 0.014$ (or diameter $r_d \approx \theta_d \cdot R \approx 1.4 \cdot 10^4$ cm). Again, the magnetic flux conservation argument leads to $B_s/B_d = (\theta_{s2}^2 - \theta_{s1}^2)/\theta_d^2 = (0.037^2 - 0.031^2)/0.014^2 = 0.48$, thus B_s is about $0.5B_d$ within the ring of the open field lines (thus $|B_m|/B_d \sim 1.6$ in this region). The actual values of surface magnetic field (radial B_r^s and total $B^s = \sqrt{(B_r^s)^2 + (B_\theta^s)^2}$) are shown as solid lines in the lower panel of Fig. 3, in comparison with radial components of dipolar field B_d (dashed horizontal line). As one can see, $B_r^s < B_r^d = 2m \cos\theta/R^3$ and B_r^s is negative for $|\theta| < 0.022$. If the dipolar surface component of pulsar magnetic field $B_d \sim 7 \times 10^{13}$ G (like in PSR J1726–3530, Table 1), then the actual surface magnetic field $B_s \sim 4 \times 10^{13}$ G, below the photon splitting threshold.

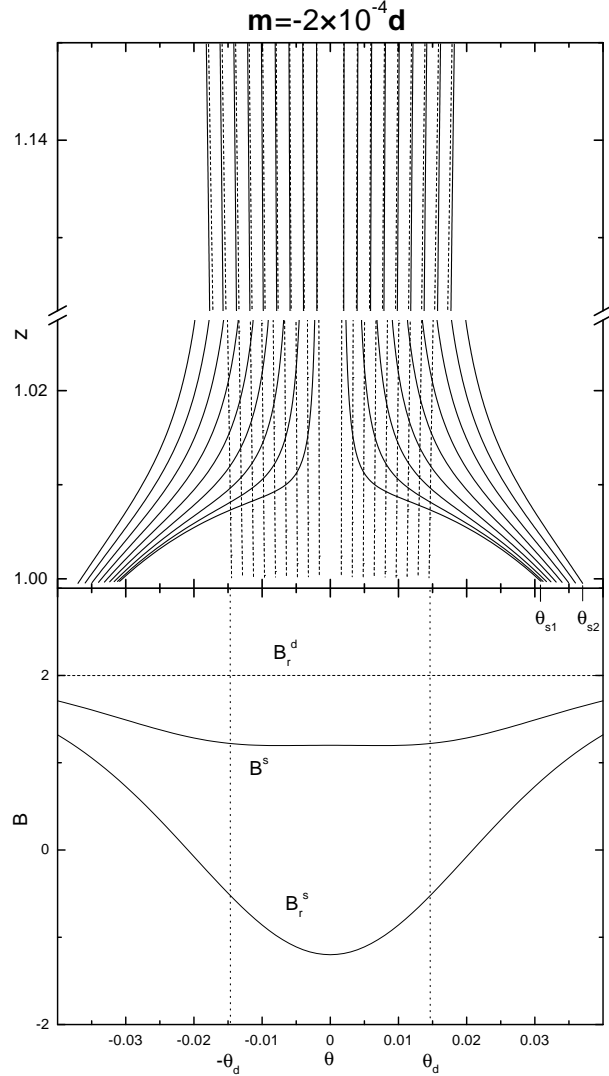


Fig. 3. As in Fig. 2 but for $\mathbf{m} = -2 \times 10^{-4}\mathbf{d}$.

2.2. Normal pulsars

Fig. 4 presents a case with $\mathbf{m} = 2 \times 10^{-4}\mathbf{d}$ in which both magnetic moments have the same polarity. Obviously in such case, the surface magnetic field will be stronger as compared with pure dipole ($m = 0$). Flux conservation argument gives surface magnetic field $B_s/B_d = (\theta_d/\theta_s)^2 = (0.014/0.008)^2 \sim 3$ (the ration $B_m/B_d \lesssim 2 \times 10^{-4}8000 = 1.6$). Thus the actual surface field is about 3 times stronger than the inferred dipolar field $B_p = 6.4 \times 10^{19}(P \cdot \dot{P})^{1/2}$ G. It is interesting to compare this case with the previous one ($\mathbf{m} = -2 \times 10^{-4}\mathbf{d}$ presented in Fig. 3), in which the actual surface field B_s is about 2 times weaker than the global dipolar surface field at the polar cap. Such cases of increasing an effective magnetic field can be important in normal pulsars with low dipolar field $B_d \ll 10^{13}$ G (Gil & Mitra, 2001).

It is then interesting to examine how different polarities of \mathbf{d} and \mathbf{m} would influence normal pulsars with

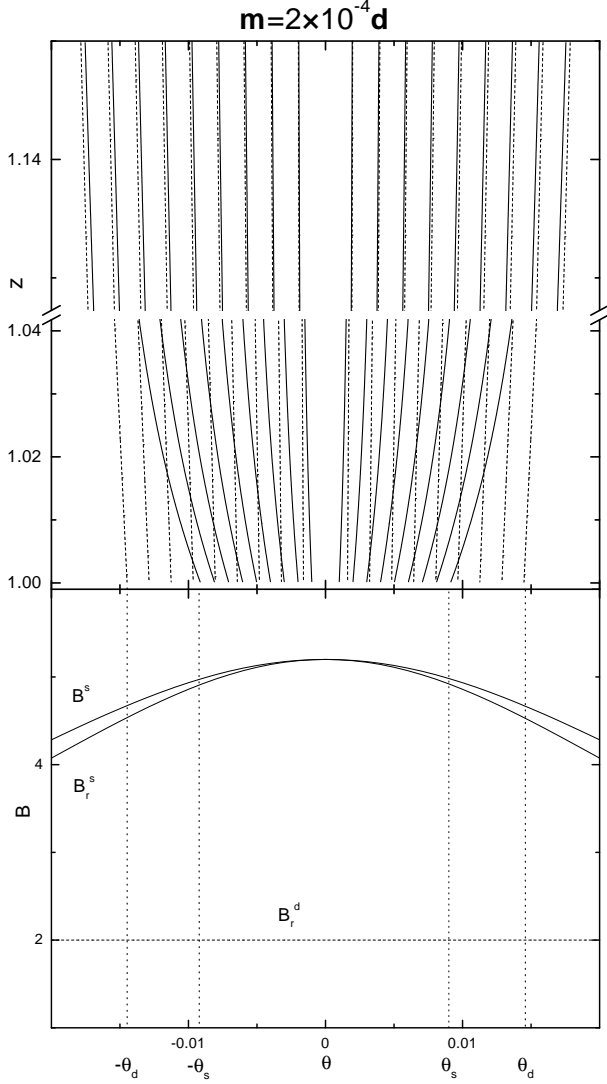


Fig. 4. As in Fig. 3 but for $\mathbf{m} = 2 \times 10^{-4} \mathbf{d}$.

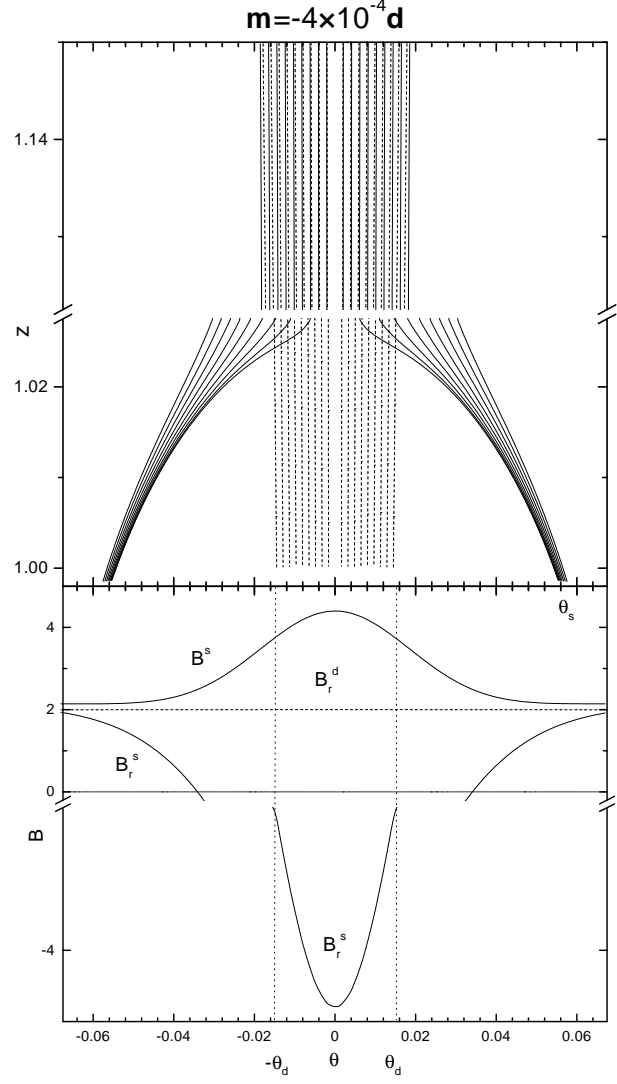


Fig. 5. As in Fig. 4 but for $\mathbf{m} = -4 \times 10^{-4} \mathbf{d}$.

$B_d \ll B_{cr}$. If $m/d \sim (\Delta R/R)^3$ thus $B_m \sim B_d$ then of course B_s can be slightly lower than B_d , as in the case of HBPs (Fig. 2). In such case, however, the VG cannot form. In fact, as argued by Gil & Mitra (2001), the formation of VG requires that B_s is close to 10^{13} G or even above, thus $B_m \gg B_d$ is required in normal pulsars (see also Gil et al. 2001). Fig. 5 illustrates a case of high surface magnetic field with $B_m \gg B_d$, in which VG can apparently form. As one can see from this figure, the values of B_s at the ring-shaped polar cap are close to dipolar values $B_s = B_d(r = R, |\theta| \sim 0.05)$. One can show that this is a general situation, that is $B_s \sim B_d$ no matter how much B_m exceeds B_d at the pole. This follows from the fact that the angular location θ of the polar cap ring increases with the increasing ratio $B_m/B_d \approx (m/d)(\Delta R/R)^3 \simeq 8 \times 10^3 (m/d)$. For example, in the case presented in Fig. 5 $\mathbf{m} = -4 \times 10^{-4} \mathbf{d}$ (thus for $\Delta R = 0.05R$ we have $B_m \sim 3B_d$ at the pole) and the last open field lines emanate at polar angles $\theta_s \approx \pm 0.055$ radi-

ans, or at polar cap radii $R_p \sim 6 \times 10^4$ cm (for $P = 1$ s). Thus, the narrow polar cap ring is located far from the local dipole \mathbf{m} , whose influence is weak at this distance. The circumpolar field lines between polar angles -0.053 to $+0.053$ are closed.

Thus, we conclude that the actual pulsar surface magnetic field B_s can significantly differ (say by an order of magnitude) from the inferred dipolar field B_d only in the case when the polarities of the global \mathbf{d} and local \mathbf{m} dipole (Fig. 1) are the same, as illustrated in Fig. 4. If this is the case, then B_s can largely exceed B_d , which seems to be important from the viewpoint of vacuum gap formation requiring $B \gtrsim 10^{13}$ G (see Gil & Mitra, 2001). Therefore, in normal VG driven radio pulsars the polar cap should be circular, or at least filled - if the axial symmetry does not hold. The ring-shaped polar cap can occur only in normal pulsars with $B_d \lesssim B_{cr}$ and in radio-loud HBPs with $B_d \gtrsim B_{cr}$.

Gil et al. (2001) explored consequences of the vacuum gap model interpretation for drifting subpulses observed in PSR B0943+10, in which 20 sparks move circumferentially around the perimeter of the polar cap, each completing one circulation in 37 pulsar periods (Deshpande & Rankin, 1999, 2001). Gil et al. (2001) considered both the curvature radiation (CR) and resonant inverse Compton radiation (ICS), seed photons as sources of electron-positron pairs and determined the parameter space for the surface magnetic field structure in each case. For the CR-VG the surface magnetic field strength $B_s > 2 \times 10^{13}$ G and the radius of curvature of surface field lines $0.6 \times 10^5 \text{ cm} < \mathcal{R} < 1.2 \times 10^5 \text{ cm}$, while for the resonant ICS-VG $B_s > 2 \times 10^{13}$ G and $10^6 \text{ cm} < \mathcal{R} < 3 \times 10^6 \text{ cm}$ (of course, in both cases $B_s < B_q \sim 4.4 \times 10^{13}$ G). The CR-VG with such curved surface magnetic field does not seem likely (although it cannot be excluded), while the ICS-VG gap supported by the magnetic field structure determined by the parameter space determined above guarantees a system of 20 sparks circulating around the perimeter of the polar cap by means of the $\mathbf{E} \times \mathbf{B}$ drift in about 37 pulsar periods.

Further Gil et al. (2001) modelled the magnetic field structure determined by the ICS-VG parameter space (specified above), using the numerical formalism developed in this paper. Since $B_d = 6.4 \times 10^{12} (P \cdot \dot{P})^{1/2} \text{ G} = 4 \times 10^{12}$ G in this case, then to obtain $\mathbf{B}_s \sim (2 \div 3) \times 10^{13}$ G one needs $B_m \gg B_d$ and the same polarity of both components. Following the symmetry suggested by the observed patterns of drifting subpulses in PSR B0943+10, the local dipole axis was placed at the polar cap center. A number of model solutions corresponding to $r_s \sim 0.97$ and $m \sim (1 \div 2) \times 10^{-4}$ d and satisfying the ICS-VG parameter space, was then obtained. As a result of this specific modelling Gil et al. (2001) obtained a number of interesting and important conclusions: (i) The conditions for the formation of the ICS-VG are satisfied only at peripheral ring-like region of the polar cap, which can just accommodate a system of 20 $\mathbf{E} \times \mathbf{B}$ drifting sparks. (ii) The surface magnetic field lines within the actual gap are converging, which stabilizes the $\mathbf{E} \times \mathbf{B}$ drifting sparks by preventing them from rushing towards the pole (as opposed to the case of diverging dipolar field (e.g. Fillipenko & Radhakrishnan, 1982)). (iii) No model solutions with $B_s \sim (3 \div 4) \times 10^{13}$ G and $\mathcal{R} \sim (0.6 \div 1.2) \times 10^5$ cm, could be obtained which corresponding to the CR-VG parameter space, which in turn favors the ICS-VG in PSR B0943+10.

3. Discussion and conclusions

We argue in this paper that a putative presence of strong non-dipolar magnetic field on the neutron star surface can help to understand recently discovered radio pulsars with magnetic field above the photon splitting threshold, as well as to understand long standing problems of the vac-

uum gap formation and drifting subpulse phenomenon. We model the actual surface magnetic field as the superposition of the global star-centered dipole and local crust-anchored dipoles $\mathbf{B}_s = \mathbf{B}_d + \sum_i \mathbf{B}_{mi} \approx \mathbf{B}_d + \mathbf{B}_{mo}$, where \mathbf{B}_{mo} is the local dipole nearest to the polar cap centre (Fig. 1). Such model is quite general, as it describes the magnetic field structure even if the star-centered dipole is negligible at the star surface. In such a case the surface dipole field \mathbf{B}_d (inferred from P and \dot{P} measurements) is a superposition of all crust-anchored dipoles calculated at far distance and projected down to the polar cap surface according to the dipolar law.

We propose a model for radio-loud HBP with high inferred dipolar magnetic field $B_d > 10^{13}$ G, even exceeding the critical value $B_{cr} \sim 4 \times 10^{13}$ G. Given the difficulty that at strong magnetic field the magnetic pair creation process is largely suppressed, the puzzling issue remains how these HBPs produce their e^-e^+ pair plasma necessary for generation of the observable radio emission. Zhang & Harding (2000a) proposed a “lengthened version” of the stationary SCLF model of inner accelerator (e.g. Arons & Shareman, 1979), in which the pair formation front occurs at altitudes r high enough above the polar cap that $B_d \sim B_{cr}(R/r)^3$ degrades below B_{cr} , thus evading the photon splitting threshold. Our VG model is an alternative to the lengthened SCLF model, with pair creation occurring right at the polar cap surface, even if magnetic field exceeds B_{cr} . We have assumed that the open surface magnetic field lines result in an actual pulsar from superposition of the star centered global dipole moment and a crust anchored local dipole moment. We argued that if the polarities of these two components are opposite, and their values are comparable, then the actual value of the surface magnetic field B_s can be lower than the critical field B_{cr} , even if the global dipole field B_d exceeds the critical value. Thus, the creation of electron-positron plasma is possible at least over a part of the polar cap and these high magnetic field neutron stars can be radio-loud (HBPs). In fact, one should expect that in HBPs, in which by definition $B_d \gtrsim B_{cr} \sim B_q = 4.4 \times 10^{13}$ G, the ratio B_m/B_d should be of the order of unity, since $\mathbf{B}_s = \mathbf{B}_d + \mathbf{B}_m$ and $10^{13} \text{ G} \lesssim B_s \lesssim B_{cr} \sim 4 \times 10^{13}$ G.

Within our simple model of non-dipolar surface magnetic field \mathbf{B}_s one should expect that both cases $\mathbf{m} \cdot \mathbf{d} > 0$ and $\mathbf{m} \cdot \mathbf{d} < 0$ will occur with approximately equal probability. However, from the viewpoint of observable radio emission only the latter case is interesting in HBPs with $B_d \gtrsim B_{cr}$. In fact, when $\mathbf{m} \cdot \mathbf{d} > 0$ then the surface magnetic field $B_s > B_d \gg B_{cr}$ (Fig. 4) and the photon splitting level is highly exceeded. For $\mathbf{m} \cdot \mathbf{d} < 0$ we have two possibilities: (i) if $m/d \lesssim (\Delta R/R)^3$ thus $B_m \lesssim B_d$ at the pole ($r = R, \theta = 0$) then the polar cap (locus of the open field lines) is circular (Fig. 2); (ii) if $m/d > (\Delta R/R)^3$ thus $B_m > B_d$ then part of the circumpolar field lines are closed and the actual polar cap has the shape of ring (Fig. 3). In both above cases (i) and (ii), the actual sur-

face magnetic field B_s at the polar cap (or at least part of it) can be lower than B_{cr} , even if B_d exceeds B_{cr} . The values of B_m and $B_d \gtrsim B_{cr}$ should be comparable to make reduction of strong surface field B_s below B_{cr} possible. In our illustrative examples presented in Figs. 2 and 3 (corresponding to the same pulsar with $P = 1$ s and $B_d = 2dR^{-3} = 6.4 \times 10^{19}(P \cdot \dot{P})^{1/2}$ G) we used ratios B_m/B_d ranging from 0.5 to 1.6. These values could be slightly different, say by a factor of few, thus we can say that the ratio B_m/B_d should be of the order of unity. If $B_m/B_d \gg 1$, then the reduction of surface dipole field is not effective (see example presented and discussed in Fig. 5). On the other hand, the case with $B_m \ll B_d$ is not interesting, as it represents a weak surface magnetic field anomaly. Thus, among a putative population of neutron stars with $B_d \gtrsim B_{cr}$, only those with the ratio $B_m/B_d = (m/d)(R/\Delta R)^3$ of the order of unity, and with magnetic moment \mathbf{m} and \mathbf{d} (Fig. 1) antiparallel at the polar cap surface, that is $\mathbf{m} \cdot \mathbf{d} < 0$, can be detected as HBPs. Other neutron stars from this population of high magnetic dipole field objects should be radio-quiet. This probably explains why there are so few HBPs detected.

Within the lengthened SCLF model there is an upper limit around $B_d = 2 \times 10^{14}$ G for radio-loud HBPs (ZH00, Zhang 2001). As ZH00 argued, detecting a pulsar above this limit would strongly imply that only one mode of photon splitting occurs. Without the alternative model of HBPs proposed in this paper, such detection would really have great importance for the fundamental physics of the photon splitting phenomenon. In our VG based model there is no natural upper limit for the radio-loud HBPs. However, it is known that due to the magnetic pressure the neutron star surface would tend to ‘crack’, which should occur at magnetic field strengths approaching 10^{15} G (Thompson & Duncan, 1995). It is unclear how the radio emission would be affected due to such cracking process.

To illustrate the above argument, let us consider Fig. 6 which presents yet another case of opposite polarities $\mathbf{m} = -1.25 \times 10^{-4}\mathbf{d}$. With $\Delta R/R \sim 0.05$ this gives $B_m/B_d = 1.0$ and $B_s = B_d - B_m = 0$ at the pole ($r = R, \theta = 0$). The dashed horizontal line at $B = 0.2$ in the lower panel corresponds to the surface magnetic field B_s which is 10 times weaker than the global dipole component $B_d = 2$ (not shown in the figure). Thus if, for example, $B_d = 4 \times 10^{14}$ G (well above the lengthened SCLF limit $B_d = 2 \times 10^{14}$ G; such pulsar was not observed so far), then the actual surface field B_s is well below $B_{cr} \sim 4 \times 10^{13}$ G, at least at the inner part of the polar cap between $\pm\theta_v = 0.0035$ rad. This “pair forming effective” polar cap is about 2.5 times smaller than the canonical polar cap with radius $\theta_d = 0.014$ rad, and about 7 times smaller than the entire polar cap with radius $\theta_s = 0.027$ rad. Near the last open field lines at polar angles $0.027 \gtrsim |\theta| \gtrsim 0.014$ the actual surface magnetic field B_s is only about 2 times lower than B_d , while in a narrow cir-

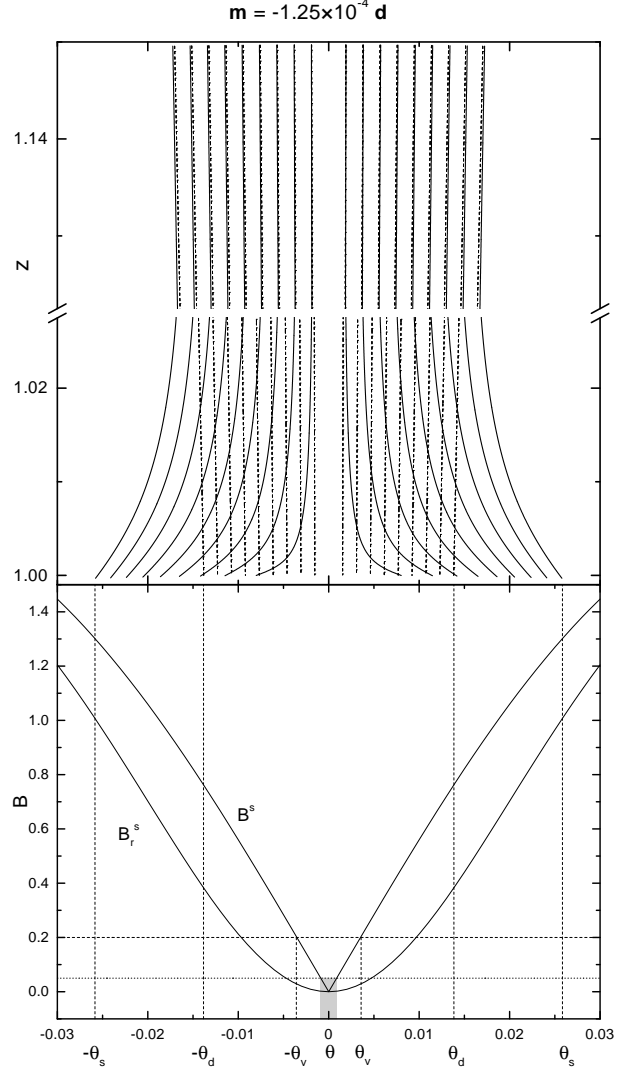


Fig. 6. As in Fig. 2 but for $\mathbf{m} = -1.25 \times 10^{-4}\mathbf{d}$. See also text for explanation.

cumpolar area with $|\theta| < \theta_v$ the surface field region B_s can be even more than 10 times weaker than B_d . Thus, within our model one can expect a radio-loud HBP with B_d even exceeding 4×10^{14} G. However, their radio-beams should be much narrower than those expected in normal pulsars, at least few to several times less than $(r_{em}/R)^{1/2}P^{-1/2}$ degrees (where r_{em} is the radio emission altitude; Kijak & Gil, 1997, 1998). This would make such sources difficult to detect.

The dotted horizontal line at $B = 0.05$ in Fig. 6 corresponds to $B_s = 10^{13}$ G for adopted $B_d = 4 \times 10^{14}$ G. This value of the surface magnetic field is believed to be about the lower limit for VG formation (see Gil & Mitra, 2001; Gil et al., 2001). Thus, the shadowed area in Fig. 6 represent a narrow hollow-cone above which the VG driven radio emission cannot occur. Similar hollow-cone is marked in Fig. 7, which presents the case similar to that illustrated in Fig. 6, except the local dipole is shifted off

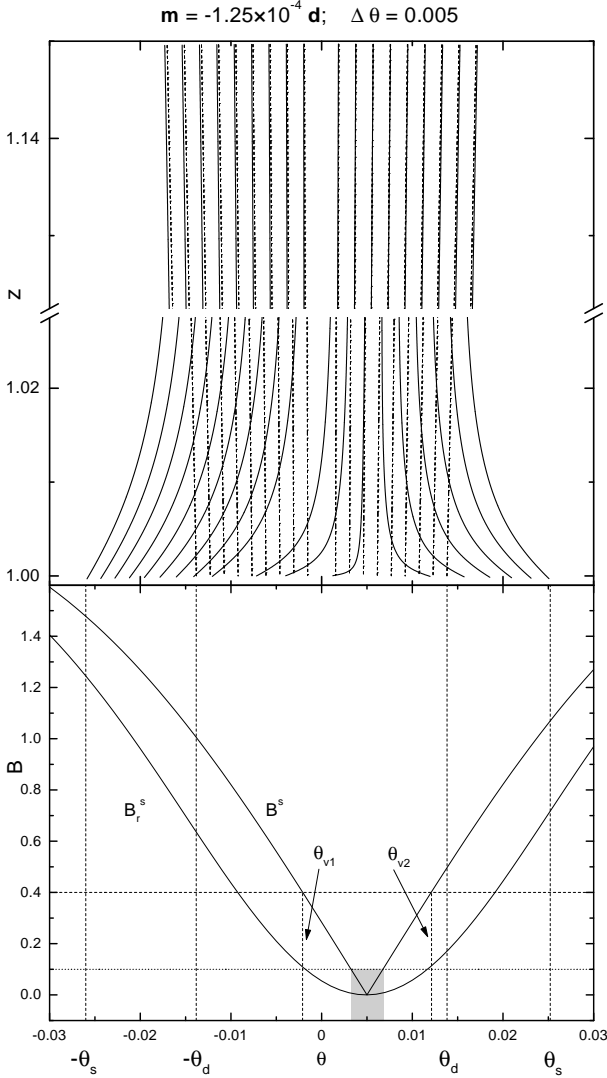


Fig. 7. As in Fig. 6 but with local dipole shifted off center by $\Delta\theta = 0.005$ radians. See also text for explanation.

center by $\Delta\theta = 0.005$ radians (corresponding to about 0.2 of the actual polar cap radius). The dashed horizontal line at $B = 0.4$ corresponds to $B_s = 4 \times 10^{13}$ G and the dotted horizontal line at $B = 0.1$ corresponds to $B_s = 10^{13}$ G, both calculated for adopted $B_d = 2 \times 10^{14}$ G. The polar angles θ_{v1} and θ_{v2} correspond to $-\theta_v$ and $+\theta_v$ in Fig. 6, respectively. The Fig. 7 demonstrates that conclusions of our paper do not depend on where the local dipole is placed.

The above arguments strengthen the possibility that some magnetars can also emit observable radio emission (Camilo et al., 2000; Zhang & Harding, 2000b). It is therefore interesting to comment on the apparent proximity of HBP PSRJ 1814–1744 (with $B_p = 1.1 \times 10^{14}$ G) and AXP 1E 2259+586 (with $B_p = 1.2 \times 10^{14}$ G) on the $P - \dot{P}$ diagram. In both these cases the inferred surface magnetic field well exceeds the critical value B_{cr} . Within our model, the former object can be radio-loud if the strong local dipole has the opposite polarity with respect to the global

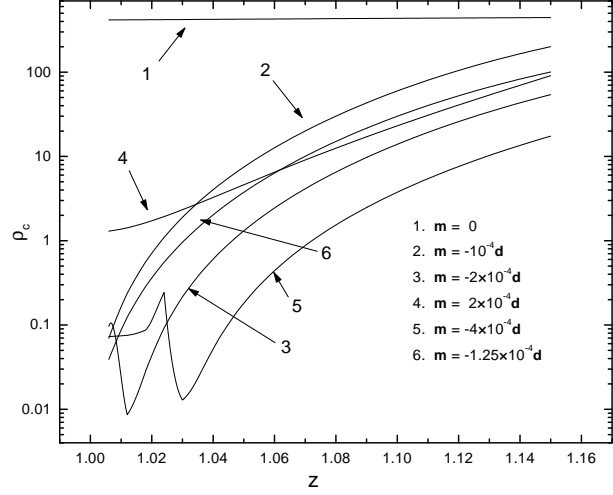


Fig. 8. Radius of curvature ρ_c (in units of $R = 10^6$ cm) as a function of normalized altitude $z = (r/R) \cdot \cos\theta$ for actual surface magnetic field lines corresponding to four cases presented in Fig. 2, 3, 4, 5 and 6. For comparison, the radius of curvature of purely dipolar field lines (in pulsar with $P=1$ s) is shown (line 1).

one. The radio quiescence of the latter object can be naturally explained if the local dipole is not able to decrease the inferred dipole magnetic field below the photon splitting death-line. Thus, either the polarities are the same or they are opposite but the local dipole is not strong enough to reduce the dipole surface field below B_{cr} .

In Fig. 8 we show the radii of curvature of actual surface field lines compared with those of purely dipolar field (line 1) as a function of normalized altitude $z = (r/R) \cos\theta$ above the polar cap. Within the polar gap at $z < 1.01$ (within about 100 meters from the surface) the curvature radii for all cases presented in Fig. 2, 3, 4, 5 and 6 have values of the order of few hundred meters (see Urpin, Levshakov & Iakovlev, 1986), suitable for curvature radiation driven magnetic pair production ($\rho_c = 1/\mathfrak{K} < 10^6$ cm, where \mathfrak{K} is the curvature of field lines).

All model calculations performed in this paper correspond to the axisymmetric case in which one local dipole is placed at the polar cap center (except the case presented in Fig. 7). In the forthcoming paper we will consider a general, non-axisymmetric case, including more local dipoles, each with different orientation with respect to the global dipole. Although this generalization will give more realistic picture of an actual surface magnetic field, it will not change our conclusions obtained in this paper.

It should be finally emphasized that although the lengthened SCLF model for HBPs (ZH00) can solve the problem of pair creation in pulsars with surface dipole field exceeding the photon splitting threshold, it does not automatically warrants generation of the coherent radio emission of such HBPs. The problem is that unlike in

the non-stationary VG model, where the low altitude radio emission can be generated by means of two-stream instabilities (Asseo & Melikidze, 1998; Melikidze, Gil & Pataraya, 2000), the stationary SCLF inner accelerator is associated with the high altitude relativistic maser radiation (e.g. Kazbegi, Machabeli & Melikidze, 1991, 1992; Kazbegi et al., 1996). This radiation requires relatively low Lorentz factors $\gamma_p \sim 5 \div 10$ of a dense secondary plasma (e.g. Machabeli & Usov, 1989). It is not clear if such plasma can be produced within the lengthened SCLF accelerator with delayed pair formation taking place in a purely dipolar magnetic field, either by curvature radiation or by inverse Compton scattering (e.g. Zhang & Harding, 2000b) processes. Moreover, the relativistic maser coherent radio emission requires a relatively weak magnetic field in the generation region. With the surface dipole field $B_d \sim 10^{14}$ G, such low field may not exist at reasonable altitudes (about 50% of the light cylinder radius $R_L = cP/2\pi$) required by the physics of corresponding instabilities (Kazbegi, Machabeli & Melikidze, 1991, 1992; Kazbegi et al., 1996). Thus, if one assumes that the radio-loud HBPs are driven by the SCLF lengthened accelerator as proposed by ZH00, they might not be able to generate observable coherent radio emission. This contradiction seems to be a challenge for the lengthened SCLF scenario for HBPs. In our VG based model the low altitude ($r \ll R_L$) radio emission of HBPs is driven by just the same mechanism as the one most probably operating in typical radio pulsars (e.g. soliton curvature radiation proposed recently by Melikidze, Gil & Pataraya, 2000). In fact, the HBPs show apparently normal radio emission, with all properties typical for characteristic pulsar radiation (Camilo et al., 2000).

Acknowledgements. This paper is supported in part by the KBN Grant 2 P03D 008 19 of the Polish State Committee for Scientific Research. We thank E. Gil and G. Melikidze Jr. for technical help. DM would like to thank Institute of Astronomy, University of Zielona Góra, for support and hospitality during his visit to the institute, where this and the accompanying letter paper was started.

References

- Adler, S.L., Bahcall, J.N., Callan, C.G., & Rosenbluth, M.N. 1970, *Phys. Rev. Lett.*, 25, 1061
- Arons, J. 1981, *ApJ*, 248, 1099
- Arons, J. 1993, *ApJ*, 408, 160
- Arons, J., & Sharleman, E.T. 1979, *ApJ*, 231, 854
- Asseo, E., Melikidze, G. 1998, *MNRAS* 301, 59
- Baring, G.M. 2001, *astro-ph/0106161*
- Baring, G.M., & Harding, A.K. 1998, *ApJ*, 507, L55
- Baring, G.M., & Harding, A.K. 2001, *ApJ*, 547, 929
- Becker, W., & Trümper, J. 1997, *A&A*, 326, 682
- Bhattacharya, D., & Shukre, C. S. 1985, *JApA*, 6, 233
- Bialynicka-Birula, Z., & Bialynicki-Birula, I. 1970, *Phys. Rev.*, 2, 2341
- Blandford, R.D., Applegate, J.H., & Hernquist, L. 1983, *MNRAS*, 204, 1025
- Bulik, T., Meszaros, P., Woo, J., Nagase, F., & Makishima, K. 1992, *ApJ*, 395, 564
- Bulik, T., Riffert, H., Meszaros, P., Makishima, S., & Mihara, T. 1995, *ApJ*, 444, 405
- Camilo, F., Kaspi, V.M., Lyne, A.G., et al. 2000, *ApJ*, 541, 367
- Chen, K., & Ruderman, M.A. 1993, *ApJ*, 402, 264
- Cheng, K., & Ruderman, M.A. 1977, *ApJ*, 214, 598
- Cheng, K., & Ruderman, M.A. 1980, *ApJ*, 235, 576
- Cheng, K.S., Gil, J., & Zhang, L. 1998, *ApJ*, 493, L35
- Cheng, K.S., & Zhang, L. 1999, *ApJ*, 515, 337
- Cordes, J.M. 1978, *ApJ*, 222, 1006
- Cordes, J.M. 1992, in *IAU Coll. 128*, ed. T.H. Hankins, J.M. Rankin & J.A. Gil Zielona Gora: Pedagogical Univ. Press), 253
- Cordes J.M. 2001, *Nature*, 409, 296
- Deshpande, A.A., & Rankin, J.M. 1999, *ApJ*, 524, 1008
- Deshpande, A.A., & Rankin, J.M. 2001, *MNRAS*, 322, 438
- Duncan, R., & Thompson, C. 1992, *ApJ*, 392, L9
- Fillipenko, A.V., & Radhakrishnan, V. 1982, *ApJ*, 263, 828
- Geppert, U., & Urpin, V. 1994, *MNRAS*, 271, 490
- Gil, J., & Sendyk, M. 2000, *ApJ*, 541, 351
- Gil, J., & Mitra, D. 2001, *ApJ*, 550, 383
- Gil, J., Melikidze, G.I., & Mitra, D. 2001, *A&A*, submitted
- Goldreich, P., & Julian, W.H. 1969, *ApJ*, 157, 869
- Gotthelf, E.V., Vasisht, G., Boylan-Kolchin, M., & Torii, A. 2000, *ApJ*, 542, 37L
- Hillebrandt, W., & Müller, E. 1976, *ApJ*, 207, 589
- Kaspi, N.M., Manchester, R.N., Johnston, S., et al. 1996, *Astron. J.*, 111 (5), 2029
- Kazbegi, A.Z., Machabeli, G.Z., & Melikidze, G.I. 1991, *MNRAS*, 253, 377
- Kazbegi, A.Z., Machabeli, G.Z., & Melikidze, G.I. 1992, in *IAU Coll. 128*, ed. T.H. Hankins, J.M. Rankin & J.A. Gil Zielona Gora: Pedagogical Univ. Press), 232.
- Kazbegi, A.Z., Machabeli, G.Z., Melikidze, G.I., et al. 1996, *A&A*, 309, 515.
- Kijak, J. 2001, *MNRAS*, 323, 537
- Kijak, J., & Gil, J. 1997, *MNRAS*, 288, 631
- Kijak, J., & Gil, J. 1998, *MNRAS*, 299, 855
- Kössl, D., Wolff, R.G., Müller, E., & Hillebrandt, W. 1988, *A&A*, 205, 347
- Krolik, J.W. 1991, *ApJ*, 373, L69
- Machabeli, G.Z., & Usov, V.V. 1989, *Sov. Astron. Lett.* 15(5), 393
- Melikidze, G.I., Gil, J., & Pataraya, A.D. 2000, *ApJ*, 544, 1081
- Mitra, D., Konar, S., & Bhattacharaya, D. 1999, *MNRAS*, 307, 459
- Murakami, T., Kubo, S., Shibazaki, N., Takeshima, T., Yoshida, A., & Kawai, N. 1999, *ApJL*, 510, L119
- Page, D., & Sarmiento, A. 1996, *ApJ*, 473, 1067

- Pirovaroff, M.J., Kaspi, V.M., & Camilo, F. 2000, *ApJ*, 535, 379
- Rudak, B., & Dyks J. 1999, *MNRAS*, 303, 477
- Ruderman, M.A., & Sutherland, P.G. 1975, *ApJ* 196, 51
- Ruderman, M.A. 1991, *ApJ*, 366, 261
- Shapiro, S.L., & Teukolsky, S.A. 1983, *Black Holes, White Dwarfs and Neutron Stars: The Physics of Compact Objects*, New York: Wiley
- Sharleman E.T., Arons J., & Fawley W.M. 1978, *ApJ*, 222, 297
- Sturrock, P.A. 1971, *ApJ*, 164, 529
- Tauris, T.M., & Konar, S. 2001, *A&A*, 376, 543
- Thompson, C., & Duncan, R.C. 1995, *MNRAS*, 275, 255
- Thompson, C., & Duncan, R.C. 1996, *ApJ*, 473, 322
- Urpin, V. A., Levshakov, S. A., & Iakovlev, D. G. 1986, *MNRAS*, 219, 703
- Usov, V.V. 1987, *ApJ*, 481, L107
- Usov, V.V., & Melrose, D.B. 1995, *Australian J. Phys.* 48, 571
- Usov, V.V., & Melrose, D.B. 1996, *ApJ*, 463, 306
- Woltjer, L. 1964, *ApJ*, 140, 1309
- Zhang, B., & Harding, A.K. 2000a, *ApJ*, 535, L51 (ZH00)
- Zhang, B., & Harding, A.K. 2000b, *ApJ*, 532, 1150
- Zhang, B., & Harding, A.K. 2001, Proc. of “Soft Gamma Repeaters: The Rome 2000 Mini-Workshop”, eds. M.Feroci and S.Mereghetti, *Mem.S.A.It.* (ZH01); *astro-ph/0102097*
- Zhang, B. 2001, *ApJ*, 562, in press